*Contribution from the Department of Chemistry,*
*University of Virginia, Charlottesville, Virginia 22901, U.S.A.*

# A Theoretical Study of Cis-Trans Photoisomerization in the Bis(Glycinato)Platinum(II) Complex*

**F. S. Richardson, D. D. Shillady, and A. Waldrop**

*Received September 24, 1970*

*The cis→trans photoisomerization of the bis glycinato complex of $Pt^{II}$ is examined on the basis of a semi-empirical molecular orbital model. It had previously been suggested by Balzani and co-workers that the reaction coordinate for this irreversible, photoisomerization process was a torsional twist of the glycine ligands about an axis that would transform the cis isomer into the trans isomer. The electronic wave functions and energies of $Pt(gly)_2$ are computed for various geometries generated by this torsional twist operation. Two minima in the total electronic energy of the ground state are found. These are at φ (twist angle) = 0° (cis) and φ = 180° (trans), and E (cis) ≳ E (trans). A single maximum is found at φ = 90°. The lowest excited electronic state appears to have two minima, one between φ = 80° and 90°, and the other between φ = 90° and 100°. The minimum on the trans side of 90° (i.e., φ > 90°) is deeper than the one on the cis side. The calculated results indicate that the lowest excited electronic state in its ground vibrational level will overlap the upper levels of the vibronic manifold of the trans ground state, whereas overlap with vibronic levels of the cis ground state is zero or nearly so. The implications of these results with respect to the mechanism and quantum yield of the photoisomerization reaction are discussed, and it is concluded that Balzani's original hypothesis is supported by our semi-quantitative theoretical study.*

## 1. Introduction

The photochemical properties of transition metal cordination complexes have long been used in preparing the reactive intermediates employed in certain inorganic syntheses, in initiating free-radical chain reactions, in the catalyses of various organic reactions, and in studies of unusual valence states and coordination geometries of inorganic compounds. Much of the recent research in the photochemistry of coordination compounds has been directed toward elucitading the stoichiometry of the photochemical processes and identifying the electronic excited states which are responsible for the observed photoreactions. Furthermore, substantial interest has developed in attempts to correlate the spectroscopic and bonding properties of the excited states of transition metal complexes with the detailed mechanisms of their photochemical transformations. These attempts have been primarily qualitative in nature and have met with, at best, equivocal success. The dearth of more quantitative structure-reactivity correlation studies can be attributed mostly to the lack of complete spectroscopic characterizations of the excited electronic states (i.e., transition polarizations, frequencies, and intensities), and to the lack of detailed quantum mechanical descriptions (i.e., good wave functions) of these states.

In this study we examine the irreversible cis to trans photoisomerization reaction of $Pt^{II}$-(glycinato)$_2$ in terms of a semi-empirical molecular orbital model. The model can be classified as an extended Hückel or Wolfsberg-Helmholtz model and has incorporated in it many features similar to those found in the work of Ballhausen and Gray,[1,2] Zerner, and Gouterman,[3] Cotton and Harris,[4] and Shillady.[5] The details of this model are discussed in section 3. It is clear that the wave functions obtained from any semi-empirical molecular orbital model will seldom be sufficiently good for calculating the spectroscopic properties of transition metal complexes with quantitative accuracy. It is expected, however, that calculations based on such a model can yield the following kinds of information:

(a) relative transition energies within the d→d, charge-transfer, and ligand→ligand manifolds;

(b) an indication of the extent and type of coupling between the metal orbitals and the ligand orbitals;

(c) relative magnitudes and polarizations of transition moments;

(d) sensitivity of the energy levels and the localized and delocalized orbitals to changes in the nuclear geometry of the complex.

Given this type of information, it is proposed that the photoreactive pathway of the reaction,

$$cis\text{–}Pt(gly)_2 \xrightarrow{h\nu} trans\text{–}Pt(gly)_2 \qquad (1)$$

can, in part, be elucidated.

(*) This work was supported in part by a National Science Foundation grant (CASS Institutional, 3760-2195) administered through the Center for Advanced Studies, University of Virginia.

(1) C.J. Ballhausen and H.B. Gray, *Inorg. Chem.*, *1*, 111 (1962).
(2) C.J. Ballhausen and H.B Gray, Molecular Orbital Theory, New York: W.A. Benjamin, Inc., (1964).
(3) M. Zerner and M. Gouterman, *Theoret. Chim. Acta* (Berl.), *4*, 44 (1966).
(4) F.A. Cotton and C.B. Harris, *Inorg. Chem.*, *6*, 369 (1966)
(5) D.D. Shillady, Ph.D. Dissertation, University of Virginia (1969).

Although the detailed mechanism of reaction (1) provides the primary motivation for this study, a second motivation arises from the close relationship which has been implied to exist between photoisomerization pathways and internal conversion and intersystem crossing mechanism.[13]

## 2. Background

In the recent development of the photochemistry of coordination compounds, square-planar $d^8$ complexes have become increasingly popular as systems for study.[6,7,8,9,10,11,12] Most of the cis-trans isomers of $d^8$ square-planar complexes that have been isolated are compounds of $Pt^{II}$ since these systems are relatively inert (compared to the analogous compounds of $Pd^{II}$ and $Ni^{II}$). Both the thermal- and the photo-isomerizations of *cis*-Pt(gly)$_2$ to *trans*-Pt(gly)$_2$ have been extensively investigated experimentally, and mechanisms for these two reactions have been proposed.[7,8,10]

Balzani, Scandola and co-workers[7,8,10] have reported that when aqueous solutions of *cis*-Pt(gly)$_2$ are heated (at 95°) in the absence of free glycine, no isomerization to the trans isomer can be detected even after 100 hr of heating. However, when free glycine was present in the solutions, they reported that about 15% of the starting cis isomer was converted to the trans isomer under the same experimental conditions. When aqueous solutions of the *cis* isomer were irradiated at 313 nm or at 254 nm, the *cis-trans* isomerization reaction proceeded both in the absence of and in the presence of free glycine. The quantum yields were reported[7] to be $0.13 \pm .01$ (313 nm) and $0.12 \pm .01$ (254 nm), and they were found to be independent of whether free glycine was present or not. Furthermore, when the thermal and photoinduced isomerization reactions were carried out in the presence of labeled free glycine, it was found that the *trans* product of the thermal isomerization contained labeled glycine whereas the *trans* product obtained from the photoisomerization contained no labeled glycine.

From these studies it was concluded that the *cis*→*trans* thermal isomerization reaction occurs by an intermolecular mechanism since: (a) the presence of free glycine is required; and, (b), the coordinated glycinato ligands are found to exchange with the free labeled glycines. An intermolecular mechanism for the photoisomerization reaction was ruled out on the basis of: (a) the constant value of the quantum yield with or without free glycine present; and,, (b), the lack of any labeled glycine in the trans product when the reaction is carried out in the presence of labeled free glycine. Furthermore, an intramolecular mechanism in which metal-ligand bonds are broken and reformed was considered unlikely since, in such a case, the reactive amino groups of the free glycines might be expected to favorably compete with the carboxyl groups for the coordination sites made vacant by metal-carboxyl bond cleavages. It was concluded that the *cis*→*trans* photoisomerization reaction takes place by a molecular twisting mechanism in which metal-ligand coordination is retained at all points along the reaction coordinate. Balzani, *et al.*, further postulated that the photoisomerization proceeded by the following steps in the case of irradiation at 313 nm:

(a) photoexcitation of the *cis* isomer to a spin-allowed d–d state which undergoes a complete deactivation to the lowest triplet excited electronic state of the complex;

(b) relaxation of the excited electronic state to its lowest vibrational level where the complex is presumed to have a slightly distorted tetrahedral geometry;

(c) intersystem crossing from the vibrationally relaxed excited state (of distorted tetrahedral symmetry) to the vibrationally excited levels of the ground electronic state of the *trans* isomer;

(d) vibrational relaxation of the ground electronic state of the *trans* isomer.

A schematic representation of this postulated reaction pathway is shown in Figure 1. In Figure 2 the nuclear geometries of the complex at several points along the reaction coordinate are depicted. The reaction coordinate is, of course, the angle of twist which transforms *cis*-Pt(gly)$_2$ into *trans*-Pt(gly)$_2$.

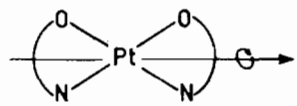


Axis about which one of the Pt(gly) chelate rings is rotated by 180°

Since this reaction is photo-irreversible (*i.e.*, the *trans*→*cis* photoisomerization is not observed), it is a necessary feature in the proposed mechanism that the equilibrium geometry of the vibrationally relaxed excited state be « distorted tetrahedral » rather then tetrahedral. That is, the minimum on the excited state potential hypersurface, with respect to the twist coordinate, φ, must be displaced towards the *trans*

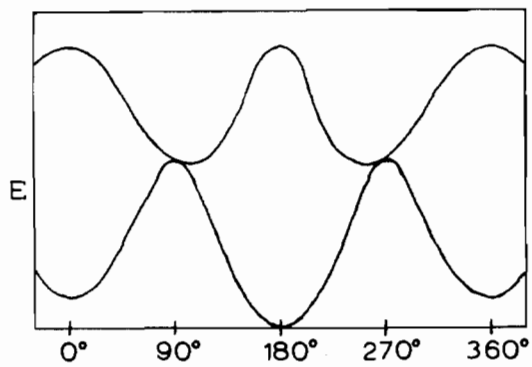


Figure 1. Schematic representation of the potential energy curves for the ground and first excited states of Pt(gly)$_2$ as postulated by Balzani, et. al. (*J. Phys. Chem.*, *72* 382 (1968)).

(6) F. Scandola, O. Traverso, and V. Carassiti, *Mol. Photochem.*, *1*, 11 (1969).
(7) V. Balzani, V. Carassiti, F Scandola, and L. Moggi, *Inorg. Chem.*, *4*, 1243 (1965).
(8) F. Scandola, O. Traverso, V. Balzani, G. Zucchini, and V. Carassiti, *Inorg. Chim. Acta*, *1*, 76 (1967).
(9) J.R. Perumareddi and A. Adamson, *J. Phys. Chem.*, *72*, 414 (1968).
(10) V. Balzani and V Carassiti, *J. Phys. Chem.*, *72*, 383 (1968).
(11) P. Haake and T.A. Hylton, *J. Am. Chem. Soc.*, *84*, 3774 (1962).
(12) L. Moggi ,F. Bolletta, V. Balzani, and F. Scandola, *J. Inorg. Nucl. Chem.*, *28*, 2589 (1966).
(13) G. Hammond, in *Advances in Photochemistry*, Vol 7, pp. 373-391; New York: Interscience Publishers (1969).

geometry ($\varphi > 90°$, if $\varphi = 0$ for *cis*, $\varphi = 90°$ for tetrahedral, and $\varphi = 180°$ for *trans*). When the complex is in this distorted tetrahedral configuration, a small barrier separates it from the *cis* ground state potential surface.

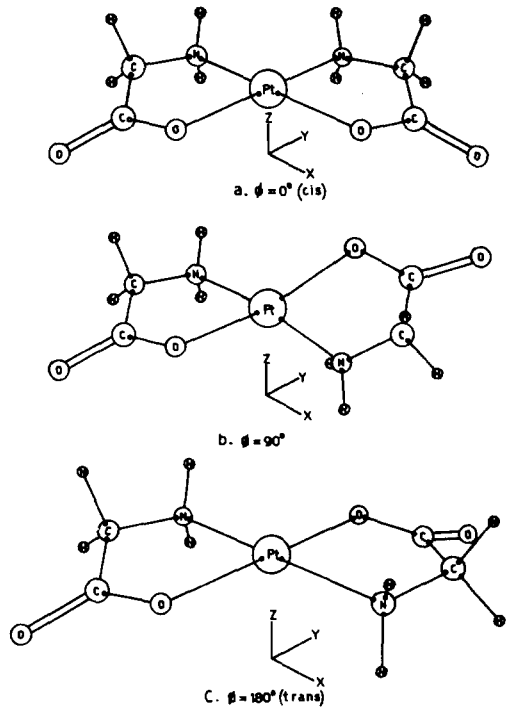


Figure 2. $Pt(gly)_2$ geometry at: a. $\varphi = 0°$ (*cis*); b. $\varphi = 90°$; c. $\varphi = 180°$ (*trans*).

The primary purpose of the present study is to examine in somewhat more semi-quantitative detail the mechanism proposed by Balzani and co-workers for the *cis*→*trans* photoisomerization of $Pt(gly)_2$. The use of a semi-empirical molecular orbital model for describing the electronic structure of the complex precludes the possibility of achieving quantitative accuracy in the calculations. However, it is reasonable to expect that the calculations can provide good qualitative or semi-quantitative tests of the proposed mechanism based on current theoretical concepts of the electronic structure of transition metal complexes.

## 3. Calculations

a. *General Procedure.* The crystal field and ligand field models, which have provided an extremely useful conceptual framework for understanding the spectroscopic properties of the essentially d→d transitions, are of little value in an analysis of properties which are intimately related to the electronic structure of the ligands or of the metal-ligand coordinate bonds. On the other hand, even a minimum basis set ab-initio SCF treatment of most transition metal complexes of chemical interest presents enormous computational problems. Furthermore, it is presently difficult to justify the time and expense required to solve these problems on the basis of improved results.

For the calculations reported here, we have adopted a semiempirical molecular orbital model which is best described as a modified extended-Huckel method. In this method a self-consistent charge calculation is first carried out on the ligands in the manner described by Duke.[14] Next the resulting diagonal energies of the ligands obtained from the last interaction of the self-consistent procedure are combined with the metal valence shell orbitals, whose VSIE's (Valence State Ionization Energies) are held constant, in a single energy minimization by solution of the secular determinant for the total system of valence shell atomic orbitals. The ligand orbitals, therefore, can adjust to the presence of the metal ion in the complex by valence shell interactions which are assumed to be proportional to overlap in the usual way.[15] This method has been previously used in calculations in the Zeise's salt anion and several hydrate, chloride, and amine complexes of $Pt^{II}$. These studies[5] indicated that the method is capable of yielding qualitatively acceptable results, and that correlations with the experimentally determined spectral properties are good.

b. *Determination of the Ligand Conformation.* In order to carry out the ligand valence shell calculation the glycinato anion conformation was needed. Since a crystal structure was not found for the $Pt^{II}$ complex, we adopted a conformation which was adjusted from the crystal structure of nickel glycine dihydrate.[15] Using the Pt–N distance of 2.16 Å from the crystal structure of *cis*-$PtCl_4 \cdot 2NH_3$[16] a local symmetry of $C_{2v}$ was assumed for the bidentate metal-ligand bonds. The Pt–O bond thus was taken to be 2.16 Å also, although subsequent adjustment of the internal bond angles in the ring led to a Pt–N distance of 2.17 Å. Then by trial and error the positions of the ligand atoms were changed until the computed angles and bond lengths fell within the limits tabulated by Freeman[17] for amino acids in metal complexes. These operations revealed that the internal angle at the alpha carbon is the most sensitive conformational parameter if one assumes planarity of the carboxyl group and that the carboxyl carbon is very nearly $sp^2$ hybridized. In effect we relaxed the $sp^3$ tetrahedral conformation at the alpha carbon somewhat and allowed the C–C–N angle to increase to 115.556° in order to keep the

**Table I.** Glycine Atomic Coordinates

| Atom | Code | X(A°) | Y | Z |
|---|---|---|---|---|
| Pt | 1 | 0.0 | 0.0 | 0.0 |
| $O^-$(Pt) | 2 | 0.181783 | 2.152337 | 0.0 |
| $C_{(0)}$ | 3 | 1.360890 | 2.542905 | —0.140227 |
| $O_{(c)}$ | 4 | 1.643194 | 3.748253 | —0.502909 |
| $C_{(\alpha)}$ | 5 | 2.496549 | 1.567959 | 0.124651 |
| $H_{(1\alpha)}$ | 6 | 3.347724 | 1.686054 | —0.545910 |
| $H_{(2\alpha)}$ | 7 | 2.922481 | 1.644697 | 1.125048 |
| N(Pt) | 8 | 2.162303 | 0.182613 | 0.0 |
| $H_{(1N)}$ | 9 | 2.537535 | —0.337575 | 0.785367 |
| $H_{(2N)}$ | 10 | 2.525356 | —0.193356 | —0.868928 |

(the second ring is formed by reflection or inversion as the case may be)

(14) B.J. Duke, *Theoret. Chim. Acta*, 9, 260 (1968).
(15) A.J. Stosick, *J. Am. Chem. Soc.*, 67, 365 (1945).
(16) R.W.G. Wyckoff, Crystal Structures, 2nd Ed., Vol 3, pp. 608-611; Interscience (1965).

**Table II.** Fitted Glycine Bond Angles

| Angle Code | Value (deg.) | Angle Code | Value (deg.) |
|---|---|---|---|
| 8,1,2 | 80.345 | 3,5,7 | 114.000 |
| 1,2,3 | 113.000 | 8,5,6 | 103.520 |
| 2,3,4 | 122.000 | 8,5,7 | 103.854 |
| 2,3,5 | 119.000 | 1,8,9 | 109.000 |
| 4,3,5 | 119.000 | 1,8,10 | 109.000 |
| 3,5,8 | 115.556 | 5,8,9 | 110.050 |
| 5,8,1 | 108.320 | 5,8,10 | 110.492 |
| 4,3,8 | 145.987 | 6,5,7 | 104.587 |
| 4,3,1 | 159.991 | 9,8,10 | 109.938 |
| 3,5,6 | 114.000 | | |

O–C–C angle near 120°. The final coordinates and some of the angles are given in Tables I and II and in Figure 3. The ring adjustment resulted in a bidentate bond angle of 80.345° with the carbonyl oxygen below the plane of the ring and the alpha carbon above. The carbonyl carbon was also placed slightly below the ring plane so that the carbonyl bond makes and angle of about 16°20′ with the O–PtN plane.

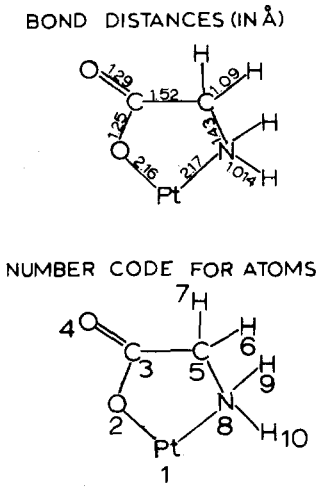


Figure 3. Bond distances and number code for atoms in $Pt(gly)_2$.

Although the conformation we have used may not be the true equilibrium geometry for the glycinato ring in this complex, we believe that it is very likely near the true conformation since the complex is undergoing thermal vibration (which we do not explicitely include in the model) at room temperature, and as long as we are within the limits given by Freemen[17] our structure is quite likely to be accessible within the manifold of allowable small deformations of the complex. On the other hand, in going from *cis* to *trans* we have used the expedient of keeping the ring conformation unchanged and varying only the angle between the two planes formed by the O–Pt–N positions. Since little is known about the conformation of the ring during this process, we can only assume that once again our assumed conformation is at least allowed if not specifically favored.

It would be interesting to monitor the photochemical isomerization by NMR techniques such as has been done by Erickson *et. al.*[18,19] for thermochemical isomerization. Perhaps there is a metastable conformation prefered in the photochemically excited state, but at this time we will assume that the ring pucker changes rapidly at room temperature so that either conformation could enter into the photo-excited state wih equal statistical weight, in which case our model is acceptable. Nevertheless one should bear in mind throughout the discussion that the twist angle which we will refer to is merely the angle between the O–Pt–N planes of two rigid ring structures.

Since the chelate rings are non-planar, we have four possible « conformational » isomers of the *cis*-$Pt(gly)_2$ complex and four possible « conformational » isomers of the *trans*-$Pt(gly)_2$ complex Four of these eight isomers are shown below:

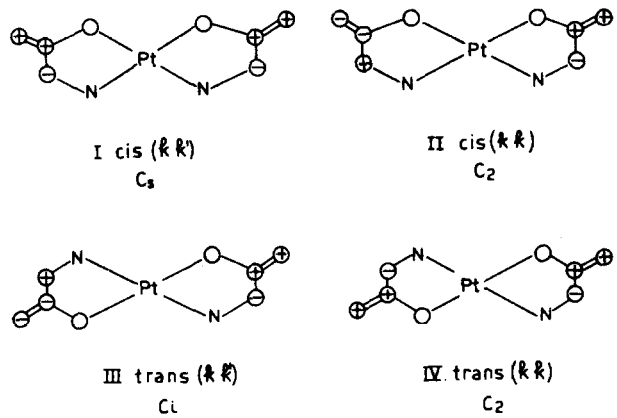


The hydrogen atoms have been omitted from these drawings, and the (+) and (−) symbols indicate whether the ligand $C_\alpha$ and C=O atoms are above or below the $PtN_2O_2$ plane, respectively. The symbols k and k′ refer to ring conformations. Note that isomers II and IV are optically active and, of course, thcir enanthiomorphs, *cis*(k′k′) and *trans*(k′k′), are also optically active. Isomers I and III are optically inactive as are *cis*(k′k) and *trans*(k′k). We performed calculations on both the *cis*(kk′) and *cis*(kk) isomers, and our results indicate that, so far as energies and intensities are concerned, the differences between their calculated properties can be neglected in this study. We obtained similar comparative results for the *trans*(kk′) and *trans*(kk) isomers.

c. *Description of the Numerical Solution.* Once the geometry of the complex was determined for any particular conformation, the calculation of the valence shell molecular orbitals was carried out using an ALGOL program (FEXTHUC) which is similar to the original Hoffman[22] program, but which has been extensively modified for ns, np, and nd orbitals using the algorithm of Lofthus and extended to include many options for off-diagonal resonance integrals and various self-consistent interaction schemes. This work was carried out by Bloor, Gilson, and Shilladv, and is discussed in reference.[5]

(17) H.C. Freeman, in Advances in Protein Chemistry, Vol. 22, pp. 257-424; New York: Academic Press (1967).

(18) L. Erickson, J. McDonald, J. Howie, and R. Crow, *J. Am. Chem. Soc.*, *90*, 6371 (1968)

(19) L. Erickson, A. Dappen, and J. Uhlenhopp, *J. Am. Chem. Soc.*, *91*, 2510 (1969).

The calculations were performed by solving the familiar equations:

$$\psi_j = \sum_i C_{ij}\Phi_i \; ; \; \Phi_i = Nr^{n-1}\exp(-\zeta_i r)Y_l^m(\theta,\varphi) \qquad (1)$$

The $\Psi_j$ functions are linear combinations of Slater type orbitals where N is a normalization constant and $\zeta_i$ is the parametric screening constant.

$$\det|H_{ij}-ES_{ij}| = O, \text{ where,} \qquad (2)$$

$$H_{ij} = \frac{kS_{ji}}{2}(H_{ii}+H_{ij}) \text{ and } S_{ij} = <\Phi_i|\Phi_j> \qquad (3)$$

In the main we have followed Cotton and Harris[4] with regard to using k = 1.8 throughout and also using their VSIE values for Pt. They have pointed out that the metal VSIE values in a complex should not vary more than about (1 ev/electron charge) in contrast to the free atom VSIE data used by Basch and Gray.[20] Since we do not iterate to self consistency for the total complex we have used their screening parameters and VSIE values for $Pt^{II}$ 5d, 6s, and 6p orbitals unchanged. The values are given in Table III.

**Table III.** Pt Extended Huckel Parameters

| Orbital | ζ | VSIE(ev) |
|---|---|---|
| Pt 5d | 3.150 | —10.61 |
| Pt 6S | 2.600 | — 9.80 |
| Pt 6P | 2.450 | — 5.35 |

For the iterative ligand calculations we have used the screening constants given by Clementi and Raimondi[21] and a value of 1.14 for hydrogen which is a compromise between 1.0 used by Hoffman,[22] when k = 1.75, and the optimum value of about 1.19 in the molecular orbital treatment of $H_2$.[23] The VSIE values were obtained from Hinze and Jaffe[24,25] and were fiitted to parabolas as described by Duke,[14] where the charges q were computed at each iteration from the usual Mulliken definitions.[26] The orbital exponents and VSIE formulas are given in Table IV. In Table V we list the last iteration diagonal matrix elements of the glycyl anion calculation which were input as VSIE values for the single iteration calculation of the bis glycyl complex.

The dipole moments and oscillator strengths were computed from the molecular orbitals obtained from the valence shell calculations and rigorous matrix elements over STOs for the dipole length operator. The original program used by Lipscomb's group was extended to handle d orbitals and the dipole moment program includes atomic polarization, charge transfer and bond moments as described by Reudenberg,[27] so that the only uncertainty in the computed results are due to the molecular orbital coefficients and not due to any approximations in the dipole moment formulas.

Although it is well known that the oscillator strengths obtained from crude wave functions with the dipole length operator are usually too large, the polarizations and relative magnitudes can be very useful for interpretation of U. V. spectra by elimanating interpretations whose spectral polarizations and intensities do not match the experimental quantities. We used a small computer program written by Bloor and Shillady[5] to estimate oscillator strengths from the dipole length in atomic units.

**Table IV.** Ligand Orbital Extended Huckel Parameters

| Orbital | | VSIE(ev) |
|---|---|---|
| C(2s) | 1.6083 | —21.010—12.06q +0.040q² |
| C(2p) | 1.5679 | —11.270—11.795q—0.865q² |
| O(2s) | 2.2458 | —36.070—16.485q+1.145q² |
| O(2p) | 2.2265 | —18.530—15.410q—0.028q² |
| N(2s) | 1.9237 | —26.920—13.895q—1.025q² |
| N(2p) | 1.9170 | —14.420—13.075q—1.195q² |
| H(1s) | 1.14 | —13.605—12.855q |

**Table V.** Last Iteration Diagonal Elements for Glycyl Anion

| Orbital | VSIE (calc.) |
|---|---|
| $O^-$ (2s) | —26.7264 |
| $O^-$ (2p) | —10.1983 |
| O (2s, C=O) | —26.4298 |
| O (2p, C=O) | — 9.9462 |
| C (2s, C=O) | —22.0030 |
| C (2p, C=O) | —12.2473 |
| $C_\alpha$ (2s) | —21.4996 |
| $C_\alpha$ (2p) | —11.7504 |
| N (2s) | —23.5229 |
| N (2p) | —11.2377 |
| $H_\alpha$ (1s) | —14.1990 |
| $H_\alpha$ (1s) | —14.2383 |
| $H_N$ (1s) | —14.6824 |
| $H_N$ (1s) | —14.6824 |

$$<\mu|\vec{r}|\nu> = [\sum_{i<j}^{N}\sum_{\mu}^{A}\sum_{\nu}^{A}(\vec{R_i}-\vec{R_j})S_{\mu\nu}/0.529167] + <\mu|\vec{r}|\nu> \qquad (4)$$

$$<i|\vec{M}_1|j> = \sum_i^N\sum_j^N\sum_\mu^A\sum_\nu^A C_{i\mu}C_{j\nu}<\mu|\vec{r}|\nu> \qquad (5)$$

$$<i|\vec{M}_2|j> = \sum_{i\neq j}^{N}\sum_{\mu}^{A}\sum_{\nu}^{A} C_{i\mu}C_{j\nu}S_{\mu\nu}\vec{R}_j/0.529167 \qquad (6)$$

$$<i|\vec{M}_3|j> = \sum_P^N\sum_\mu^A C_{i\mu}C_{j\mu}\vec{R}_P/0.529167 \qquad (7)$$

$$<i|M|j> = \sum_{k=1}^{3}<i|\vec{M}_k|j> \qquad (8)$$

$$f_{i^j} = 3.037148\times10^{-6}E_{i^j}|<i|\vec{M}|j>|^2 \qquad (9)$$

In the formulas given above N is the number of nuclei and A is the number of atomic orbitals. The vectors $\vec{R}_i$ are the nuclear positions in angstroms and r refers to electronic coordinates in atomic units; the $C_{ij}$ values are the atomic orbital coefficients j in the molecular orbital i. The transition energies $E_i^j$ were taken to be the extended Huckel energy difference between orbitals i and j in kilokaysers. In the pro-

(20) H. Basch and H. Gray, *Inorg. Chem.*, 6, 365 (1966).
(21) E. Clementi and D. Raimondi, *J. Chem. Phys.*, 38, 2686 (1963).
(22) R. Hoffmann, *J. Chem. Phys.*, 39, 1397 (1963).
(23) J.C. Slater, Quantum Theory of Matter, 2nd Ed., Chapter 21, McGraw-Hill (1968).
(24) J. Hinze and H. Jaffe, *J. Phys. Chem.*, 67, 1501 (1963).
(25) J. Hinze and H. Jaffe, *J. Am. Chem. Soc.*, 84, 540 (1962).
(26) R.S. Mulliken, *J. Chem. Phys.*, 23, 1833 (1955).
(27) K. Ruedenberg, *Rev. Mod. Phys.*, 34, 326 (1962).

gram we use, the vector quantities $\langle i | \vec{M} | j \rangle$ were also given by components in cartesian coordinates in order to asses the polarization of the transition in question. The calculation is straightforward once the $\langle \mu | \vec{r} | \nu \rangle$ matrix elements over atoms taken two at a time are shifted to a common coordinate system and stored as $\langle \mu | \vec{r}' | \nu \rangle$ values.

## 4. Results

We calculated the molecular orbital wave functions, orbital energies, Mulliken overlap populations, orbital charges, and atomic charges for the following twist angles: $\varphi = 0°$ (*cis*), 45°, 80°, 90° (pseudo-tetrahedral), 100°, 120°, 120°, 135°, and 180° (*trans*). The static electric dipole moments, electric dipole transition moments, transition energies, and oscillator strengths were calculated for the *trans* ($\varphi = 180°$) and *cis* ($\varphi = 0°$) isomers. In Table VI the highest occupied and the lowest unoccupied molecular orbitals for the cis complex are listed along with their energies and an identification of their principal atomic orbital or bonding make-up. In Table VII a similar listing is given for the molecular orbitals of the trans complex.

**Table VI.** Cis-Molecular Orbitals

| Highest Filled Orbitals | | | |
|---|---|---|---|
| Orbital | Energy (e.v.) | Description | $C_{2v}$ Symmetry Type |
| $\psi_1$ | −9.6679 | non-bonding carbonyl | $b_2$ |
| $\psi_2$ | −9.6915 | non-bonding carbonyl | $a_1$ |
| $\psi_3$ | −9.8815 | $\pi^0$ carboxyl | $a_2$ |
| $\psi_4$ | −9.9078 | $\pi^0$ carboxyl | $b_1$ |
| $\psi_5$ | −10.0262 | $\sigma^*$Pt-carboxyl | $a_1$ |
| $\psi_6$ | −10.1335 | $\sigma^*$Pt-carboxyl | $b_2$ |
| $\psi_7$ | −10.4612 | $d_{xy} + d_{z^2}$ | $a_1$ |
| $\psi_8$ | −10.5885 | $d_{xy} - d_{z^2}$ | $a_1$ |
| $\psi_9$ | −10.6031 | $d_{yz} + d_{xz}$ | $a_2$ |
| $\psi_{10}$ | −10.6263 | $d_{yz} - d_{xz}$ | $b_1$ |

| Lowest Unfilled Orbitals | | | |
|---|---|---|---|
| Orbital | Energy (e.v.) | Description | $C_{2v}$ Symmetry Type |
| $\psi_1'$ | −7.5533 | $d_{x^2-y^2} + \sigma^*$Pt−O$^-$ | $b_2$ |
| $\psi_2'$ | −7.0720 | $\pi^*$ carboxyl | $b_1$ |
| $\psi_3'$ | −7.0242 | $\pi^*$ carboxyl | $b_1$ |

Table VIII lists the orbital and atomic electron populations for Pt, N, $C_\alpha$, C (carbonyl carbon), O (carbonyl oxygen), and $O^-$ (ligating oxygen) at seven values of the twist angle $\varphi$. The total electronic ground state energies calculated for the various values of $\varphi$ are given in Table IX.

Our molecular orbital model may be too crude to permit the use of the computed transition energies and transition dipole moments in making spectral assignments. In general, extended Hückel or Wolfsberg-Helmholz models are useful for this purpose only after extensive calibration calculations have been done in order to optimize the parameters (especially our interaction parameter in equation 3) for predicting selected spectral properties.[3,28,29] Our orbital excitation energies can be used, however, to determine in a qualitative way how the energies of certain excited state configurations vary with $\varphi$. A calculated orbital excitation energy in our model corresponds roughly to an « average » of the transition energies to the singlet and triplet partners of an excited configuration. From Tables VI and VII it can be seen that the energy gaps calculated for several ligand-to-metal charge transfer transitions are considerably smaller than those calculated for the lowest-lying d→d transitions. Furthermore, the computed charge-transfer transition energies are somewhat lower than can be supported by the available experimental data. Ligand-to-metal charge transfer will lead to considerably increased d–d repulsion energies which will push the charge-transfer excited states to higher energy. It is fairly certain that if these repusions were adequately represented in our model, the excited charge-transfer states would be pushed above the excited d→d states in energy. The transition energies we calculate are just excitation energies to virtual orbitals of the ground state and do not include such electron repulsions. Our calculations should, however, accurately predict the relative ordering of states within the d→d manifold and within the charge-transfer manifold for various values of $\varphi$.

**Table VII.** Trans-Molecular Orbitals

| Highest Filled Orbitals | | | |
|---|---|---|---|
| Orbital | Energy (e.v.) | Description | $C_{2h}$ Symmetry Type |
| $\psi_1$ | −9.6742 | non-bonding carbonyl | $b_u$ |
| $\psi_2$ | −9.6828 | non-bonding carbonyl | $a_g$ |
| $\psi_3$ | −9.8228 | $\pi^0$ carboxyl | $b_g$ |
| $\psi_4$ | −9.9705 | $\pi^0$ carboxyl | $a_u$ |
| $\psi_5$ | −9.9876 | $\sigma^*$Pt-carboxyl | $b_u$ |
| $\psi_6$ | −10.1798 | $\sigma^*$Pt-carboxyl | $a_g$ |
| $\psi_7$ | −10.4680 | $d_{z^2} + d_{xy}$ | $a_g$ |
| $\psi_8$ | −10.5009 | $d_{xz}$ | $b_g$ |
| $\psi_9$ | −10.7015 | $d_{yz}$ | $b_g$ |
| $\psi_{10}$ | −10.7651 | $d_{z^2} - d_{xy}$ | $a_g$ |

| Lowest Unfilled Orbitals | | | |
|---|---|---|---|
| Orbital | Energy (e.v.) | Description | $C_{2h}$ Symmetry Type |
| $\psi_1'$ | −7.6242 | $d_{x^2-y^2} + \sigma^*$Pt−O$^-$ | $a_g$ |
| $\psi_2'$ | −7.0523 | $\pi^*$ carboxyl | $b_g$ |
| $\psi_3'$ | −7.0298 | $\pi^*$ carboxyl | $a_u$ |

The energies of the d-orbitals in the *cis* complex are calculated to be in the following order:
$d_{x^2-y^2} \gg d_{xy} > d_{z^2} > d_{xz} = d_{yz}$.
The true symmetry of the *cis* isomer is $C_s$; however, if we consider only the $PtO_2N_2$ cluster, the effective symmetry is $C_{2v}$. We shall find it convenient to designate the molecular orbitals which have mostly d-orbital character by the irreducible representations under which they transform in the $C_{2v}$ point group.

(28) H. Basch, A. Viste, and H. Gray, *J. Chem. Phys.*, *44*, 10 (1966).
(29) F. Cotton, C. Harris, and J. Wise, *Inorg. Chem.*, *6*, 909 (1967).

**Table VIII.** Orbital and Atomic Electron Populations Versus φ

| Atom | Orbital | 0° | 45° | 80° | 90° | 100° | 135° | 180° |
|---|---|---|---|---|---|---|---|---|
| | 6s | 9.8354 | 9.8555 | 9.9225 | 9.9890 | 9.9462 | 9.8808 | 9.8576 |
| | $6p_z$ | 0.7279 | 0.6959 | 0.6659 | 0.6655 | 0.6688 | 0.7028 | 0.7352 |
| | $6p_x$ | 0.0183 | 0.0597 | 0.1386 | 0.0774 | 0.1363 | 0.0561 | 0.0184 |
| | $6p_y$ | 0.1745 | 0.1833 | 0.1929 | 0.2427 | 0.1998 | 0.2004 | 0.1923 |
| | $5d_{z^2}$ | 0.1745 | 0.1758 | 0.1647 | 0.2007 | 0.1637 | 0.1646 | 0.1579 |
| | $5d_{xz}$ | 1.8819 | 1.9376 | 1.9628 | 1.9630 | 1.9614 | 1.9356 | 1.8823 |
| | $5d_{yz}$ | 1.9965 | 1.9083 | 1.7697 | 1.5160 | 1.7676 | 1.8970 | 1.9988 |
| | $5d_{x^2-y^2}$ | 1.9965 | 1.8777 | 1.7352 | 1.4744 | 1.7621 | 1.9023 | 1.9944 |
| | $5d_{xy}$ | 0.8743 | 1.0446 | 1.3473 | 1.9073 | 1.3423 | 1.0495 | 0.8874 |
| Pt | | 1.9909 | 1.9727 | 1.9454 | 1.9421 | 1.9441 | 1.9727 | 1.9909 |
| $O^-$ | | 6.0986 | 6.0858 | 6.0482 | 6.0036 | 6.0247 | 6.0542 | 6.0679 |
| O(Carbonyl) | | 6.5495 | 6.5436 | 6.5200 | 6.5030 | 6.5186 | 6.5452 | 6.5466 |
| C(Carbonyl) | | 3.9432 | 3.9400 | 3.9460 | 3.9471 | 3.9460 | 3.9440 | 3.9429 |
| $C_\alpha$(alpha carbon) | | 3.9807 | 3.9630 | 3.9800 | 3.9796 | 3.9798 | 3.9803 | 3.9806 |
| N | | 4.7383 | 4.7467 | 4.7730 | 4.7967 | 4.7862 | 4.7671 | 4.7601 |

**Table IX.** Total Ground State Energies (e.v.)

| φ | E(e.v.) | |
|---|---|---|
| 0° | −1092.7604 | *cis* |
| 45° | −1092.1795 | |
| 80° | −1091.1197 | |
| 90° | −1090.7046 | pseudo-tetrahedral |
| 100° | −1091.1283 | |
| 120° | −1091.7888 | |
| 135° | −1092.2025 | |
| 180° | −1092.7886 | *trans* |

Using the notation of Table VI, we have:

$$\psi_1'(b_2) = d_{x^2-y^2}$$
$$\psi_7(a_1) = (1/2)^{1/2}(d_{xy} + d_{z^2})$$
$$\psi_8(a_1) = (1/2)^{1/2}(d_{xy} - d_{z^2})$$
$$\psi_9(a_2) = (1/2)^{1/2}(d_{xz} + d_{yz})$$
$$\psi_{10}(b_1) = (1/2)^{1/2}(d_{xz} - d_{yz})$$

and the relative energies are, $\Psi_1' \gg \psi_7 > \psi_8 > \psi_9 > \psi_{10}$.

Note that, because of interactions between the two chelate rings, the two mo's which contain linear combinations of $d_{xz}$ and $d_{yz}$, are not degenerate.

First we shall examine, on the basis of our calculated results, the hypothesis that the photochemical reaction pathways is[7,8,10] *cis ground state* $\xrightarrow{h\nu}$ high vibrational level of electronic excited $\xrightarrow{VR}$ relaxed electronic excited state of distorted tetrahedral geometry $\xrightarrow{ER}$ trans ground state. In this scheme, VR = vibrational relaxation processes within an electronic state; and ER = radiationless electronic relaxation processes (*i.e.*, internal conversion or intersystem crossing processes) between electronic states. In simplest terms this reaction pathway should be promoted by any event or sequence of events that: (a) increases electron density in the regions between the metal atom and the N and $O^-$ ligating atoms in the *cis* complex (*i.e.*, along the x and y axes); and, (b) creates a hole (decreases electron density) in those regions in which the metal-ligand bonds exist in the pseudo-tetrahedral (φ = 90°) complex. The lobes of the $d_{x^2-y^2}$ orbital point directly toward the four ligating atoms in the *cis* complex, but only toward two of the ligating atoms in the pseudo-tetrahedral complex (since we only rotate one ligand group in generating the tetrahedral complex). The lobes of the $d_{xz}$ and $d_{yz}$ orbitals do not point directly at any ligating atom in the *cis* complex, but do point directly at two ligating atoms in the pseudo-tetrahedral complex. One might expect, therefore, that an excitation to the $\Psi_1'$ mo (which is principally $d_{x^2-y^2}$ and anti-bonding between Pt and the ligands) would weaken the σ-bonding structure of the complex. Furthermore, excitation out of the $\psi_9$ or $\psi_{10}$ mo's (principally of $d_{xz}$ and $d_{yz}$ character) would create a hole in regions where the ligating atoms are located in the pseudo-tetrahedral complex.

The mo's with large d-orbital coefficients are antibonding with respect to the Pt-ligand bonds. Furthermore, the absolute magnitude of the overlap between a d-orbital and the orbitals on the ligating atoms is a rough measure of the antibonding character in the corresponding mo's. The larger the absolute overlap, the larger the antibonding character in the mo, and the higher the energy. In Table X we list the total absolute overlaps between the metal d-orbitals and the orbitals on the ligating atoms for φ = 0°, 80°, 90°, 100°, and 180°. «Total absolute overlap» is defined as

$$S_m = \sum_L [\sum_i |S_{im}|]$$

where m denotes d-orbital, L denotes ligating atoms, and i labels the valence orbitals (2S, $2P_x$, $2P_y$, $2P_z$) on each ligating atom. From Table X we see that the largest variations in the total d-orbital-ligand orbital overlaps as a function of φ occur for the $d_{x^2-y^2}$, $d_{xz}$, and $d_{yz}$ orbitals. These results indicate that the $d_{xz}$ and $d_{yz}$ orbitals should increase in energy in going from φ = 0 to φ = 90°, whereas the $d_{x^2-y^2}$ orbital should

**Table X.** Total Aboslute Overlaps

| φ = | 0° | 80° | 90° | 100° | 180° |
|---|---|---|---|---|---|
| $d_{x^2-y^2}$—$L_4$ | .8218 | .5630 | .5093 | .5630 | .8218 |
| $d_{xy}$—$L_4$ | .3168 | .4588 | .4693 | .4588 | .3168 |
| $d_{z^2}$—$L_4$ | .4650 | .3930 | .4002 | .3930 | .4650 |
| $d_{xz}$—$L_4$ | .0983 | .4215 | .4365 | .4341 | .1114 |
| $d_{yz}$—$L_4$ | .0983 | .4210 | .4234 | .4215 | .0852 |

decrease in energy. For the twist angles, $\varphi=45°$, 120°, and 135°, it is nearly impossible to make correlations between the *cis* mo's and mo's of equivalent atomic orbital contributions in the twisted complexes. However, for $\varphi=80°$, 90°, and 100°, very close correlations can be made between the *cis* $\psi_1'(d_{x^2-y^2})$, $\psi_9(d_{xz}+d_{yz})$, and $\psi_{10}(d_{xz}-d_{yz})$ mo's and their equivalents (*i.e.*, equivalent with respect to atomic orbital make up) in the twisted complexes. For the $\psi_7$ and $\psi_8$ *cis* mo's, only very crude correlations can be made since the $d_{z^2}$ and $d_{xy}$ orbitals enter strongly into three or four mo's of the twisted systems.

**Table XI.** Orbital Energies (e.v.)

| MO* | φ 0° | 80° | 90° | 100° |
|---|---|---|---|---|
| $\psi_1'(b_2)$ | —7.5533 | —8.8539 | —9.0432 | —8.8578 |
| $\psi_9(a_2)$ | —10.6031 | —9.2176 | —9.0392 | —9.2196 |
| $\psi_{10}(b_1)$ | —10.6263 | —10.6183 | —10.6190 | —10.6114 |

* $C_{2v}$ Symmetry Designation.

**Table XII.** Energy Gaps (e.v.)

| | φ 0° | 80° | 90° | 100° |
|---|---|---|---|---|
| $\psi_9 \rightarrow \psi_1'$ | 3.0498 | 0.3937 | —0.0040 | 0.3518 |
| $\psi_{10} \rightarrow \psi_1'$ | 3.0730 | 1.7744 | 1.5758 | 1.7536 |

In Table XI, the energies of the *cis* $\psi_1'$, $\psi_9$, and $\psi_{10}$ mo's are compared with their equivalents at $\varphi=80°$, 90°, and 100°. The $\psi_1' \rightleftarrows \psi_9$ and $\psi_1' \leftrightarrows \psi_{10}$ energy gaps are given in Table XII. Note that the$\psi_1'$ mo has a lower energy than does the $\psi_9$ mo at 90°. This result indicates that the $(\psi_9\ \psi_1')$ excited state configuration is more stable than the $(\psi_9)^2$ configuration at $\varphi=90°$. Furthermore, it appears that the $(\psi_9\ \psi_1')$ excited state has an energy minimum somewhere close to $\varphi=90°$. The $\psi_{10}$ mo also increases in energy as φ is increased from 0°, but it never approaches the energy of $\psi_1'$ and the $(\psi_{10}\ \psi_1')$ excited state configuration has a somewhat higher energy than does $(\psi_{10})^2$ at $\varphi=90°$. The mo's of the twisted isomers which correlate most closely with the $\psi_7$ and $\psi_8$ *cis* mo's remain at somewhat lower energies than $\psi_1'$. If we further approximate the energies of the excited state configurations, $(\psi_9\ \psi_1')$ and $(\psi_{10}\ \psi_1')$, by adding the excitation energies of the processes, $\psi_9 \rightarrow \psi_1'$ and $\psi_{10} \rightarrow \psi_1'$, respectively, to the computed ground state energies, we obtain the results shown in Table XIII. The values given in Table XIII represent very crude approximations to the true excited state energies since they are obtained by using the calculated excitation energies to virtual orbitals of the ground state. However, since they represent excited states within the d→d manifold, their relative magnitudes are probably useful.

The more usual method of Mulliken overlap population analysis was carried out for each conformation of the complex, but since the excited states which are important in the reaction mechanism are not occupied in the ground state, the usual bonding definitions

**Table XIII.** Approximate Excited State Configuration Energies

| E(e.v.) | 0° | 80° | 90° | 100° |
|---|---|---|---|---|
| $E_9(\psi_9\psi_1')$ | —1089.7106 | —1090.7260 | —1090.7086 | —1090.7765 |
| $E_{10}(\psi_{10}\psi_1')$ | —1089.6874 | —1089.3453 | —1089.1288 | —1089.3747 |

**Table XVI.** Reduced Overlap Populations *

| φ= | 0° | 80° | 90° | 100° | 180° |
|---|---|---|---|---|---|
| Pt-O | 0.3086 | 0.2724 | 0.2998 | 0.2799 | 0.3051 |
| Pt-N | 0.3663 | 0.3390 | 0.3541 | 0.3376 | 0.3691 |
| (Pt-N)+(Pt-O) | 0.6749 | 0.6114 | 0.6539 | 0.6175 | 0.6742 |

* see reference [26] for definition.

do not elucidate the photochemistry. Nevertheless, one interesting ground state feature which we observed is presented in Table XIV. If we consider only the metal-ligand bonds we see that there is a metastable bonding maximum at about $\varphi=90°$. Equating bond strength with overlap population we might also point out a slight asymmetry in the bonding favoring the trans side of the distorted tetrahedral conformation. Although this effect is certainly small, it does reinforce the photochemical mechanism toward the trans isomer. This asymmetry is probably not as important as that in the excited states however.

At this point we can review our evidence for the existance of an excited electronic state whose equilibrium geometry is near tetrahedral (energy minimum near $\varphi=90°$), and whose potential surface along the φ coordinate crosses or nearly crosses the ground state surface. The following results are considered:

(a) Table VIII. The combined electron population of the $d_{xz}$ and $d_{yz}$ orbitals decreases from 3.99 at $\varphi=0°$ to 2.99 at $\varphi=90°$. The electron population of $d_{x^2-y^2}$ increases from 0.87 at 0° to 1.91 at 90°. These results indicate that the tetrahedral configuration is made most stable by shifting an electron from the $d_{xz}$, $d_{yz}$ orbital pair to the $d_{x^2-y^2}$ metal orbital. Furthermore, since the total charge on Pt changes by only 0.16 on going from 0° to 90°, metal-ligand charge transfer appears to be unimportant in stablizing the tetrahedral configuration. In fact, the relative charge densities on the metal and ligands remain nearly constant over the entire variation of φ from 0° to 180°.

(b) Tables XI and XII, Figure 4. The energy of $\psi_9(a_2)$ increases as φ is increased from 0° to 90°, and then begins to decrease for $\varphi>90°$. The energy of $\psi_1'(b_2)$ decreases from $\varphi=0°$ to $\varphi=90°$ and then increases for $\varphi>90°$. The energy levels of $\psi_9(a_2)$ and $\psi_1'(b_2)$ cross somewhere close to $\varphi=90°$.

(c) Table XIII, Figure 5. These results must be used with some caution. The two upper curves in Figure 5 are not sections through the true potential energy surfaces of excited states $(\psi_9\ \psi_1')$ and $(\psi_{10}\ \psi_1')$, but the qualitative features of the curves should be similar to those of the true excited state energy curves along the φ coordinate. $E_9(\varphi)$ appears to be a double-minima function over the interval, $\varphi=0°$ to 180°, and it intersects the groundstate «energy sur-

face» near $\varphi=90°$. The two minima in $E_9(\varphi)$ are asymmetric. If we take the minima to be located at $\varphi=80°$ and 100°, and the maximum at $\varphi=90°$, the barrier heights for the two minima are: 80°, $\Delta E=0.0174$ e.v.; 100°, $\Delta E=0.0679$ e.v.

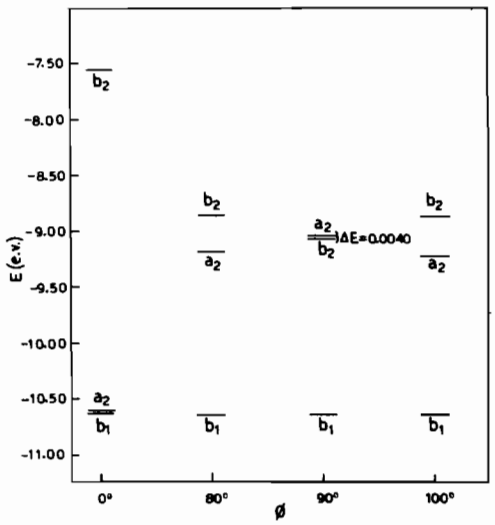


Figure 4. Energy level diagram for $\psi_9(b_1)$, $\psi_{10}(a_2)$, and $\psi_1'(b_2)$ molecular orbitals as function of $\varphi$. Symmetry designations refer to *cis* ($C_{2v}$) parentage.

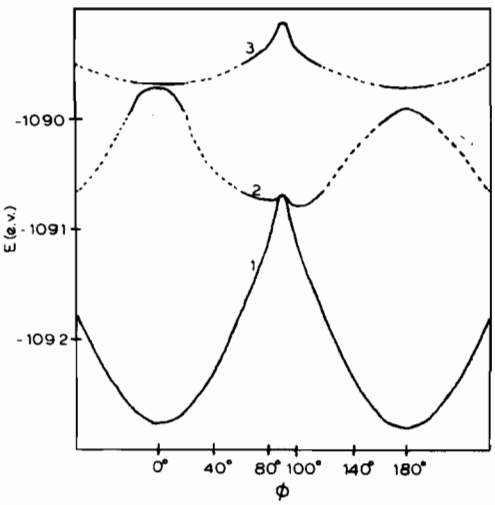


Figure 5. Total electronic energy versus twist angle $\varphi$
1. Ground State
2. Excited State ($\psi_{10}$ $\psi_1'$)
3. Excited State ($\psi_9$ $\psi_1'$)

These results indicate that once the *cis* complex gets into the ($\varphi_9$ $\psi_1'$) excited state, either by direct excitation or by ER (where ER refers to either internal conversion or intersystem crossing) from other excited states, there exists a direct pathway for transformation to the *trans* isomer. The minimum in $E_9(\varphi)$ on the trans side of the pseudo-tetrahedral geometry (i.e., the one near $\varphi=100°$) is deeper than the minimum on the *cis* side (i.e., the one near $\varphi=80°$). This suggests that in the vibrationally relaxed ($\psi_9$ $\psi_1'$) state, the complex already has a tetrahedrally distorted *trans* geometry. Furthermore, since $E_9(\varphi)$ intersects the ground state energy surface on either side of $\varphi=90°$, radiationless conversion to the *trans* ground state from ($\psi_9$ $\psi_1'$) should be very efficient. The barrier height between the minima in $E_9(\varphi)$ is rather small however, so one might also expect ER to the *cis* ground state to be non-negligable. This competition between ER processes to the *cis* and *trans* ground states might explain, in part, why the quantum yield for the reaction is $<1.0$. In order for electronic relaxation to the *cis* ground state to be competitive with similar processes leading to the *trans* ground state, the barrier height on the *cis* side of 90° must be larger than the zero-point energy of the twisting mode in the ($\psi_9$ $\psi_1'$) excited state. If the zero-point energy is larger than the barrier height on the *cis* side but smaller than the barrier height on the *trans* side (as appears to be the case), then internal conversion to the *trans* isomer is highly favored. This would also make the photoisomerization reaction irreversible.

So far we have discussed only the ($\psi_9$ $\psi_1'$) and ($\psi_{10}$ $\psi_1'$) excited states in detail. The remaining two d→d excited states, ($\psi_7$ $\psi_1'$) and ($\psi_8$ $\psi_1'$), do not approach the ground state energy surface along $\varphi$ and are not strong candidates for the mediating excited state in the isomerization reaction. Excitation out of the $d_{xy}$ and $d_{z^2}$ orbitals does not significantly decrease the energy of the intermediate tetrahedral complex. Similar arguments can be given to eliminate the charge-transfer states as important in providing a low energy path from *cis* to *trans*. The low-lying charge-transfer transitions transfer electron density into the $d_{x^2-y^2}$ orbital and thereby weaken the metal-ligand $\sigma$-bond system. However, this process merely creates a «hole» on the ligands and should have little influence on distortions or rearrangements in the metal-ligating atom cluster. As mentioned earlier, a ligand→metal charge-transfer process will significantly increase the energy of the charge-transfer state. Since these repulsions are completely ignored in our model, it is expected that excitation energies for charge-transfer transitions which are calculated by taking differences between the orbital energies of Table VI will be much too small.

## 5. Discussion

Our results suggest a mechanism for the *cis*→*trans* photoisomerization of $Pt((gly)_2$ which is similar to the one first proposed by Balzani, *et al.*[7] We have further identified the excited state which mediates the transformation. This state arises from the excitation, ($d_{xz}$ + $d_{yz}$)→$d_{x^2-y^2}$, and has a distorted tetrahedral equilibrium geometry. The potential energy surface of this excited state intersects the surfaces of the other low lying excited states along the twist coordinate $\varphi$, and intersects the ground state energy surface near $\varphi=90°$. Excitations to the other excited states can, therefore, be followed by rather efficient radiationless electronic relaxation processes which lead to the mediating state and finally to the *trans* ground state. Our calculations suggest that the energy of the mediating state $E(\varphi)$ is a double-minima function along $\varphi$ with a shallow minimum on the *cis* side of $\varphi=90°$, and a deeper minimum on the *trans* side.

This study has concentrated primarily on using a «computational model» for examining the electronic aspects of the *cis*→*trans* photoisomerization of $Pt(gly)_2$. It is of some interest, however, to consider the mechanism or pathway of this reaction on the basis of a more formal theoretical approach. We consider such an approach only very briefly here.

Consider the following schematic representation of the events which might occur in the course of the

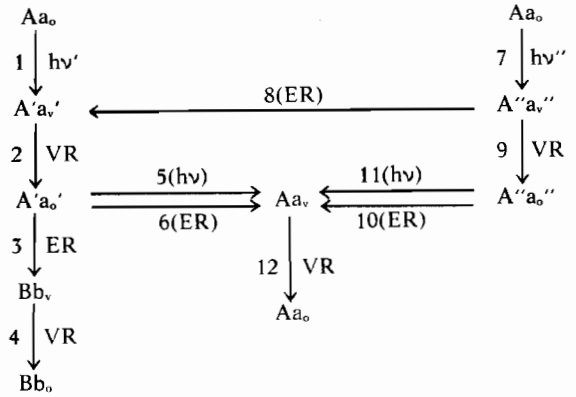


In this schematic, ER and VR denote radiationless electronic and vibrational relaxation processes, respectively, and hν denotes radiative processes (absorption or emission). $Aa_o$ represents the ground electronic state of the cis isomer in its ground vibrational level, $A'a_v'$ and $A''a_v''$ represent excited electronic states, A' and A'', of the *cis* isomer in their vth vibrational levels $a_v'$ and $a_v''$, respectively, and $Bb_v$ represents the ground electronic state of the *trans* isomer in its vth vibrational level.

Since the *cis*-$Pt(gly)_2$ complex does not exhibit luminescence, processes 5 and 11 need not be considered further. If we excite directly into the A' state, then the probable sequence of events in the isomerization reaction is 1→2→3→4. The quantum yield for the reaction is determined by the competition of this sequence of events with the sequence: 1→2→6. The latter sequence yields a *cis* product. More specifically, the relative probabilities of processes 3 and 6 determine the yield for the *cis*→*trans* isomerization. Processes 3 and 6 proceed by ER mechanisms. If we assume that the ER processes are made possible by resonance or near-resonance interactions between the connecting vibronic states, then the transition probabilities for processes 3 and 6 can be written as:

$$T_3 = \langle A'a_o'|H'|Bb_v\rangle^2 \qquad (10)$$

$$T_6 = \langle A'a_o'|H'|Aa_v\rangle^2 \qquad (11)$$

where H' is a perturbation operator. H' is defined by

$$H' = H - H_o \qquad (12)$$

where H is the total Hamiltonian of the system and $H_o$ is the zeroth-order Hamiltonian which neglects both spin-orbit and vibronic interactions. The states A, A', and B are assumed to be eigenstates of $H_o$. If we further assume that H' depends only upon electron coordinates,[30,31] then equations (10) and (11) can be expressed as:

$$T_3 = \langle A'|H'|B\rangle^2\langle a_o'|b_v\rangle^2 = \beta_3\langle a_o'|b_v\rangle^2 \qquad (13)$$

$$T_6 = \langle A'|H'|A\rangle^2\langle a_o'|a_v\rangle^2 = \beta_6\langle a_o'|a_v\rangle^2 \qquad (14)$$

where $\beta_3$ and $\beta_6$ now denote the electronic integrals.

If $\beta_3 = \beta_6$, then the transition probabilities $T_3$ and $T_6$ are related by

$$T_3/T_6 = \langle a_o'|b_v\rangle^2 / \langle a_o'|a_v\rangle^2, \qquad (15)$$

and the quantum yield of the isomerization reaction will depend on the relative magnitudes of the Franck-Condon overlap integrals, $\langle a_o' \mid b_v \rangle$ and $\langle a_o' \mid a_v \rangle$. The results reported in Section 4 indicate that the mediating excited state (corresponding to the state A' in the present discussion) has two minima on its total energy surface along the coordinate φ, and that the minimum on the trans side of $\varphi = 90°$ is somewhat deeper than the minimum on the *cis* side. This suggests that $\int a_o' b_v d\varphi > \int a_o' a_v d\varphi$, and that $T_3 > T_6$. To a good approximation, $\beta_3$ will be equal to $\beta_6$ so long A' is essentially a d→d excited state, since in this case:

$$\beta_3 = \langle d'|H'|d_{x^2-y^2}\rangle \qquad (16)$$

$$\beta_6 = \langle d'|H'|d_{x^2-y^2}\rangle \qquad (17)$$

where d' represents a «hole» orbital in the excited state A', and $d_{x^2-y^2}$ is the «hole» orbital in both A and B.

An example of a purely electronic perturbation H' would be the spin-orbit interaction operator. This perturbation would be effective in coupling the singlet ground states, $^1A$ and $^1B$, with a triplet excited state $^3A'$. If we consider H' to be a vibronic Hamiltonian and express it to first-order in the twist coordinate φ, then

$$H' = \varphi(\partial H/\partial\varphi)_{\varphi=90°} = \varphi H'_e \qquad (18)$$

Now H' depends upon both the electron coordinates and the nuclear coordinates (through φ). The differential operator $H'_e$ is evaluated at $\varphi = 90°$ and operates only upon electron coordinates. In this case the transition probabilities, $T_3$ and $T_6$, are related in the following way:

$$T_3/T_6 = \langle a_o'|\varphi|b_v\rangle^2 / \langle a_o'|\varphi|a_v\rangle^2. \qquad (19)$$

Again, our results from section 4 suggest that $T_3 > T_6$. The vibronic perturbation will be effective in coupling the singlet ground states, $^1A$ and $^1B$, with a singlet excited state $^1A'$.

So far we have assumed that H' is a «stationary» intramolecular perturbation that couples the vibrationally relaxed excited state $A'a_o'$ with the vibronic components, $Aa_v$ and $Bb_v$, of the *cis* and *trans* ground electronic states. If H' is assumed to be stationary and $A'a_o'$ is in resonance or near-resonance (i.e., nearly isoenergetic) with $Aa_v$ and $Bb_v$, then the internal conversion processes 3 and 6 will not go. Instead, the system will merely undergo oscillations between the connecting states. We shall not discuss this problem any further here except to say that several corrections and additions to the model have been presented which would force the system to proceed to

complete electronic and vibrational relaxation. The most complete and fundamental treatment has been given by Jortner, Rice, and Hochstrasser.[32] Robinson and Frosch[30,31] assume that H′ is stationary, but they also postulate interactions between the vibronic states of the isolated system and lattice vibrations of the solvent medium. These solute-solvent interactions are necessary in order to drive the electronic relaxation processes to completion.

Our calculations suggest that the isomerization process (process 3) takes place through a single channel; that associated with the twist coordinate φ. However, it is rather unlikely that ER to the *cis* ground state (process 6) occurs exclusively through this channel. In fact it is more probable that this electronic relaxation process occurs mainly through channels provided by skeletal stretching modes in the $PtO_2N_2$ cluster. Taking this into consideration, the quantum yield for the *cis*→*trans* photoisomerization reaction can be expressed as follows:

$$(QY)=\frac{T_3(\varphi)}{T_3(\varphi)+T_6(\varphi)+\sum_i T_6(Q_i)} \tag{20}$$

where $\Sigma_i$ is taken over all vibrational modes $Q_i$ of the *cis* complex except the twist mode φ. Equation 20 applies only to the case in which the initial excitation is from state A to state A′. If we excite directly into a higher excited state, say A″, then processes 8, 9, and 10 must be considered explicitly. Balzani, *et. al.*[10] reported quantum yields of 0.12 and 0.13 at 254 nm and 313 nm, respectively. This suggests that the transition probability of process 8 is nearly unity. In writing down equation 20 we ignored any external quenching effects which might result from couplings between solvent electronic states and the electronic states of the complex. In aqueous solutions these effects can be safely neglected.

For the reverse reaction, *trans*→*cis* photoisomerization, the quantum yield expression is:

$$(QY)'=\frac{T_3'(\varphi)}{T_3'(\varphi)+T_6'(\varphi)+\sum_j T_6'(Q_j')} \tag{21}$$

where $\sum_j$ is taken over all vibrational modes $Q_i'$ of the *trans* complex except the twist mode φ, and the transition probabilities are given by,

$$T_3'=\langle B'b_o'|H'|Aa_v\rangle^2 \tag{22}$$

$$T_6'=\langle B'b_o'|H'|Bb_v\rangle^2 \tag{23}$$

B′ is the first excited state of the *trans* complex. Assuming that B′ correlates with A′ (at least along the φ coordinate), then $T_3'(\varphi)\approx T_6(\varphi)$ and $T_6'(\varphi)\approx T_3(\varphi)$. Balzani, *et. al.*[10] reported that $(QY)'=0$ for all excitation wavelengths in the d→d spectral region, and that $(QY)=0.13$ for irradiation at 313 nm. These observations, can be explained in several ways:

(a) If $T_6'(Q_j')$ is very large ($\approx 1$) for one or more modes, then ER processes from B′ to B are highly favored over the B′→A processes.

(b) If $T_3(\varphi)\gg T_6(\varphi)$, then the B′→B and A′→B processes are favored over the B′→A and A′→A processes.

Our calculations indicate that $T_3(\varphi)>T_6(\varphi)$; but the difference in their magnitudes is probably not sufficient to preclude an observable quantum yield for the *trans*→*cis* isomerization. The irreversibility is probably due, therefore, to the existence of very efficient ER channels (other than along φ) between B′ and B. Furthermore, the low quantum yield of the *cis*→*trans* isomerization suggests that the A′ state can relax to the *cis* ground state A more efficiently through some mode $Q_i$ than through φ. The selection rules which govern the electronic integrals in the transition probabilities, are identical in both the *cis*→*trans* and *trans*→*cis* reactions. The relative quantum yields should, therefore, be primarily controlled by Franck-Condon overlap factors.

*Acknowledgments.* We express our gratitude to Professor John Bloor for his essistance in developing parts of the molecular orbital program (FEXTHUC) used in this study. Financial support was provided by the National Science Foundation through a subgrant to F. R. administered by the Center for Advanced Studies, University of Virginia.

(30) G.W. Robinson and R. Frosch, *J. Chem. Phys.*, 37, 1962 (1962).
(31) G.W. Robinson and R. Frosch, *J. Chem. Phys.*, 38, 1187 (1963).
(32) J. Jortner, S. Rice, and R. Hochstrasser, in Advances in Photochemistry, Vol. 7, pp 149-309; New York: Interscience Publishers (1969).